J Neurophysiol
87: 889–900, 2002; 10.1152/jn.00135.2001.

Pacemaker Neurons for the Theta Rhythm and Their Synchronization in the Septohippocampal Reciprocal Loop

XIAO-JING WANG
Volen Center for Complex Systems, Brandeis University, Waltham, Massachusetts 02254-9110

Received 16 February 2001; accepted in final form 15 October 2001

Wang, Xiao-Jing. Pacemaker neurons for the theta rhythm and their synchronization in the septohippocampal reciprocal loop. *J Neurophysiol* 87: 889–900, 2002; 10.1152/jn.00135.2001. Hippocampal theta (4–10 Hz) oscillation represents a well-known brain rhythm implicated in spatial cognition and memory processes. Its cellular mechanisms remain a matter of debate, and previous computational work has focused mostly on mechanisms intrinsic to the hippocampus. On the other hand, experimental data indicate that GABAergic cells in the medial septum play a pacemaker role for the theta rhythm. We have used biophysical modeling to address two major questions raised by the septal pacemaker hypothesis: what is the ion channel mechanism for the single-cell pacemaker behavior and how do these cells become synchronized? Our model predicts that theta oscillations of septal GABAergic cells depend critically on a low-threshold, slowly inactivating potassium current. Network simulations show that theta oscillations are not coherent in an isolated population of pacemaker cells. Robust synchronization emerges with the addition of a second GABAergic cell population. Such a reciprocally inhibitory circuit can be realized by the hippocampo-septal feedback loop.

INTRODUCTION

During exploratory movements and rapid-eye movement (REM) sleep, the hippocampus exhibits a prominent coherent "theta" rhythm (4–10 Hz) (Bland 1986; Green and Arduni 1954; Stewart and Fox 1990; Vanderwolf 1969), which is often temporally nested with faster gamma-frequency (~40 Hz) oscillations (Bragin et al. 1995; Buzsáki et al. 1983; Soltész and Deschênes 1993; Stumpf 1965). The theta rhythm is believed to play a role in the hippocampal representation of spatial information (Kahana et al. 1999; O'Keefe and Recce 1993; Skaggs et al. 1996) and to facilitate the induction of synaptic plasticity (Buzsáki 1989; Huerta and Lisman 1993).

The neural mechanisms underlying the generation of the theta rhythm remain unresolved (Buzsáki 2001). Hippocampal cultures (Fischer et al. 1999) or slices (MacVicar and Tse 1989) can be induced by muscarinic activation to display coherent oscillations in the theta frequency range. Computational models have been developed for synchronized oscillations at theta frequency generated in the hippocampus (Traub et al. 1992; White et al. 2000). However, muscarinic receptor-dependent oscillations are fundamentally distinct from theta rhythm in vivo (Williams and Kauer 1997). Probably, the propensity of hippocampal networks to oscillate at theta frequency reflects a resonance mechanism (Hutcheon and Yarom 2000; Pike et al. 2000) rather than theta rhythmogenesis itself. Numerous studies showed that in the intact brain, the hippocampal theta rhythm depends critically on the integrity of the afferent inputs from the medial septum (MS) (Bland 1986; Green and Arduni 1954; Stewart and Fox 1990). For example, when hippocampal theta is abolished by fornix-fimbria lesion, rhythmic firings persist in MS cells (Andersen et al. 1979; Petsche et al. 1962; Vinogradova 1995). MS contains two major types of neurons (Brashear et al. 1986; Gritti et al. 1993) that are thought to play distinct roles in the theta rhythm generation: cholinergic cells acting via muscarinic receptors modulate slowly the excitability of hipoccampal neurons (Cole and Nicoll 1984; Gähwiler and Brown 1985), whereas GABAergic cells play a role of pacemakers via fast $GABA_A$ receptor-mediated synaptic transmission (Freund and Antal 1988; Stewart and Fox 1990). Specifically, it has been hypothesized that MS GABAergic afferents impose the θ rhythmicity on GABAergic cells in the hippocampus (Freund and Antal 1988) that in turn phasically pace the firings of pyramidal neurons (Cobb et al. 1995; Tóth et al. 1997). Several lines of evidence are in support of this scenario. First, movement-related theta rhythm was not blocked by muscarinic receptor antagonists such as atropine (Kramis et al. 1975; Vanderwolf 1969). Second, when cholinergic neurons (but not GABAergic neurons) in the MS were chemically damaged, the frequency of hippocampal theta was found to remain unchanged, but the power was dramatically reduced (Apartis et al. 1998; Lee et al. 1994), consistent with the view that cholinergic cells contribute to the theta rhythm by providing a tonic drive to the hippocampus. Third, local injection of GABA-A antagonist in MS eliminated θ rhythmicity in the putative cholinergic cells but not that in the putative GABAergic cells (as differentiated by broad vs. brief spikes, respectively) (Brazhnik and Fox 1999). This last result could be interpreted as evidence that oscillations in cholinergic cells depend on the inhibitory synaptic inputs from GABAergic pacemaker neurons.

Two critical questions remain open concerning the pacemaker hypothesis of septal GABAergic neurons: what is the ion channel mechanism for the single-cell pacemaker behavior and how do these cells become synchronized? The present work investigates these two issues using a computational approach. Recent in vitro studies have revealed that noncholinergic (putative GABAergic) neurons in the basal forebrain

Address for reprint requests: Volen Center for Complex Systems, MS 013, Brandeis University, 415 South St., Waltham, MA 02254-9110 (E-mail: xjwang@brandeis.edu).

The costs of publication of this article were defrayed in part by the payment of page charges. The article must therefore be hereby marked "*advertisement*" in accordance with 18 U.S.C. Section 1734 solely to indicate this fact.

(BF) (Alonso et al. 1996) and the MS (Serafin et al. 1996) display robust intrinsic gamma and theta oscillations that are inter-nested in time (Fig. 1*A*). Based on these slice data, we propose an ionic channel mechanism for the pacemaker properties observed in putative MS GABAergic neurons. We then consider the network synchronization both for an isolated population of MS GABAergic cells and for a reciprocally inhibitory loop between the MS and the hippocampus.

METHODS

Medial septal GABAergic neuron model

The MS neuron model is based on current-clamp data on noncholinergic (putative GABAergic) neurons in the nucleus basalis (Alonso et al. 1996) and MS (Serafin et al. 1996). Based on the TTX experiment (Serafin et al. 1996), we assume that the intrinsic membrane rhythmicity is generated by an interplay between a sodium current and a voltage-activated potassium current (Alonso and Llinás 1989; Gutfreund et al. 1995; Llinás et al. 1991; Wang 1993). Furthermore, when depolarized from hyperpolarization, these cells typically show a ramp response, with the spike discharge preceded by a delay of up to a hundred of milliseconds (Fig. 1*A*). This ramp response is taken as evidence of a potassium current I_{KS} that inactivates slowly (see RESULTS). The model includes only the minimal number of ion channels that are considered essential to account for the experimental data. It is similar to a previous model (Wang 1993), except that it does not include a separate persistent noninactivating sodium current because preliminary voltage-clamp data indicate that putative GABAergic cells in the BF and MS do not possess a large persistent sodium current (A. Alonso, personal communication). The one-compartment model contains spike-generating currents (I_{Na} and I_K), plus a slowly inactivating potassium current (I_{KS}). The membrane potential obeys the following current balance question

$$C_m dV/dt = -I_{Na} - I_K - I_{KS} - I_L - I_{syn} + I + \epsilon\eta(t)$$

where $C_m = 1\ \mu F/cm^2$, I is the injected current (in $\mu A/cm^2$). The leak current $I_L = g_L(V - E_L)$ has a conductance $g_L = 0.1$ mS/cm^2, so that the passive time constant $\tau_m = C_m/g_L = 10$ ms; and $E_L = -50$ mV. Membrane noise is introduced (for Figs. 1–3) in $\epsilon\eta(t)$, where $\eta(t)$ is uncorrelated in time, and uniformly distributed between -1 and $+1$; $\epsilon = 0.3$. The synaptic current I_{syn} represents synaptic interactions in network simulations and is specified in the following text.

The three voltage-dependent currents are described by the Hodgkin-Huxley formalism. Thus a gating variable x satisfies a first-order kinetics, $dx/dt = \phi_x[\alpha_x(V)(1 - x) - \beta_x(V)x] = \phi_x[x_\infty(V) - x]/\tau_x(V)$. The sodium current $I_{Na} = g_{Na}m_\infty^3 h(V - E_{Na})$, where the fast activation variable is replaced by its steady-state, $m_\infty = \alpha_m/(\alpha_m + \beta_m)$, $\alpha_m = -0.1(V + 33)/\{\exp[-0.1(V + 33)] - 1\}$, $\beta_m = 4\exp[-(V + 58)/18]$; $\alpha_h = 0.07\exp[-(V + 51)/10]$, and $\beta_h = 1/\{\exp[-0.1(V + 21)] + 1\}$. The delayed rectifier $I_K = g_K n^4(V - E_K)$, where $\alpha_n = -0.01(V + 38)/\{\exp[-0.1(V + 38)] - 1\}$, and $\beta_n = 0.125\exp[-(V + 48)/80]$. The temperature factor $\phi_h = \phi_n = 5$. The slowly inactivating potassium current $I_{KS} = g_{KS}pq(V - E_K)$ has a relatively low activation threshold and an inactivation time constant of ~200 ms. We have $p_\infty = 1/\{1 + \exp[-(V + 34)/6.5]\}$, $\tau_p = 6$ ms, $q_\infty = 1/\{1 + \exp[(V + 65)/6.6]\}$, and $\tau_q = \tau_{q0}(1 + 1/\{1 + \exp[-(V + 50)/6.8]\})$, $\tau_{q0} = 100$ ms. The following parameter values were used: $g_{Na} = 50$, $g_K = 8$, $g_{KS} = 12$ (in mS/cm^2); $E_{Na} = +55$, $E_K = -85$ (in mV). The resting state (with $I = 0$ and $\epsilon = 0$) is at $V = -62.5$ mV.

Hippocampo-septal neuron model

Hippocampal GABAergic neurons that project to the MS are calbindin-containing and constitute a subpopulation of cells with hori-

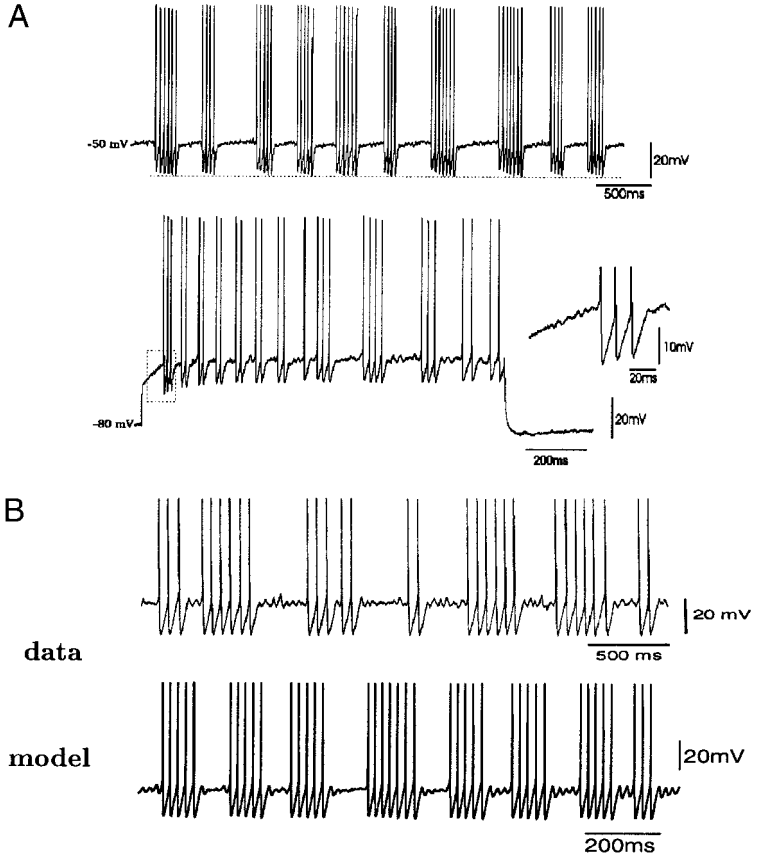

FIG. 1. *A*: characteristic electrophysiological properties of basal forebrain (BF) noncholinergic cells (reproduced with permission from Alonso et al. 1996). *Top*: spontaneous discharge in rhythmic spike "clusters" at 3 Hz (at 32°C). Note the ramp potential between spike clusters accompanied by subthreshold membrane potential oscillations. Note also the progressive increase in the spike afterhyperpolarization during the cluster. *Bottom*: delayed firing and spike clusters in response to a depolarizing current pulse applied from −80 mV. Note in the enlargement to the right the development of subthreshold oscillations during the delayed depolarization prior to spiking. *B, top*: membrane oscillation of a noncholinergic (putative GABAergic) cell in the rat medial septum (reproduced with permission from Serafin et al. 1996). *Bottom*: model simulation. The simulated oscillation is faster than the experimental data because of the temperature difference between the model simulation (for theta at body temperature) and experimental measurements (at 32°C).

zontally oriented dendrites located in stratum oriens-alveus ("horizontal O/A interneurons") (Tóth and Freund 1992). We model these cells based on physiological data from slice studies (Ali and Thomson 1998; Lacaille and Williams 1990; Maccaferri and McBain 1996). A hippocampo-septal neuron is described by a single compartment and obeys the current balance equation

$$C_m dV/dt = -I_{Na} - I_K - I_h - I_{Ca} - I_{KCa} - I_L - I_{syn} + I$$

with the same conventions as for the MS cells. The spike currents I_{Na} and I_K are identical to those used in Wang and Buzsáki (1996). The transient sodium current $I_{Na} = g_{Na} m_\infty^3 h(V - E_{Na})$, where $m_\infty = \alpha_m/(\alpha_m + \beta_m)$; $\alpha_m(V) = -0.1(V + 35)/\{\exp[-0.1(V + 35)] - 1\}$, $\beta_m(V) = 4\exp[-(V + 60)/18]$; $\alpha_h(V) = 0.07\exp[-(V + 58)/20]$, and $\beta_h(V) = 1/\{\exp[-0.1(V + 28)] + 1\}$. The delayed rectifier $I_K = g_K n^4(V - E_K)$, where $\alpha_n(V) = -0.01(V + 34)/\{\exp[-0.1(V + 34)] - 1\}$, and $\beta_n(V) = 0.125\exp[-(V + 44)/80]$. The temperature factor $\phi_h = \phi_n = 5$. The leak current $I_L = g_L(V - E_L)$.

The high-threshold calcium current I_{Ca} and the calcium-activated potassium current I_{KCa} are taken from Wang (1998) and produce spike-frequency adaptation (Ali and Thomson 1998; Lacaille and Williams 1990). The high-threshold calcium current $I_{Ca} = g_{Ca} m_\infty^2(V - V_{Ca})$, where m is replaced by its steady-state $m_\infty(V) = 1/\{1 + \exp[-(V + 20)/9]\}$. The voltage-independent, calcium-activated potassium current $I_{KCa} = g_{KCa}[Ca^{2+}]/([Ca^{2+}] + K_D)(V - V_K)$, with $K_D = 30\ \mu M$. The intracellular calcium concentration $[Ca^{2+}]$ is assumed to be governed by a leaky-integrator

$$\frac{d[Ca^{2+}]}{dt} = -\alpha I_{Ca} - [Ca^{2+}]/\tau_{Ca}$$

where $\alpha = 0.002$, so that the $[Ca^{2+}]$ influx per spike is ~200 nM (Helmchen et al. 1996). The various extrusion and buffering mechanisms are collectively described by a first-order decay process with a time constant $\tau_{Ca} = 80$ ms (Helmchen et al. 1996).

The hyperpolarization-activated current I_h was derived from Maccaferri and McBain (1996) with kinetic rates adjusted to the body temperature. $I_h = g_h H(V - E_h)$, with $H_\infty(V) = 1/\{1 + \exp[(V + 80)/10]\}$ and $\tau_H(V) = 200/\{\exp[(V + 70)/20] + \exp[-(V + 70)/20]\} + 5$. Other parameter values are: $g_L = 0.1$, $g_{Na} = 35$, $g_K = 9$, $g_h = 0.15$, $g_{Ca} = 1$, and $g_{KCa} = 10$ (in mS/cm^2); $E_L = -65$, $E_{Na} = +55$, $E_K = -90$, $E_h = -40$, $E_{Ca} = +120$ (in mV). $C_m = 1\ \mu F/cm^2$. In the absence of injected current ($I = 0$), the model neuron displays spontaneous repetitive discharges at ~6 Hz, similar to the horizontal O/A interneurons (Maccaferri and McBain 1996). With $I = -0.5\ \mu A/cm^2$, the model neuron is at rest with $V = -63.2$ mV.

Synapse and network model

The inhibitory synaptic current $I_{syn} = g_{syn} s(V - E_{syn})$, where g_{syn} is the maximal synaptic conductance, and $E_{syn} = -75$ mV is the reversal potential. The gating variable s represents the fraction of open synaptic channels. We assume that s obeys a simple two-variable kinetics (cf. Wang and Rinzel 1992) $dx/dt = \phi_{syn}[\alpha_x F(V_{pre})(1 - x) - x/\tau_x]$; $ds/dt = \phi_{syn}[\alpha_s x(1 - s) - s/\tau_s]$; with the scaling factor $\phi_{syn} = 1$, unless specified otherwise. The normalized concentration of the postsynaptic transmitter-receptor complex, $F(V_{pre})$, is assumed to be an instantaneous and sigmoid function of the presynaptic membrane potential, $F(V_{pre}) = 1/\{1 + \exp[-(V_{pre} - \theta_{syn})/2]\}$, where θ_{syn} (set to -20 mV) is high enough so that the transmitter release occurs only when the presynaptic cell emits a spike. Unless specified otherwise, $\alpha_x = \alpha_s = 1$, $\tau_x = 0.2$ ms, and $\tau_s = 10$ ms. With these parameters, the time-to-peak of a unitary postsynaptic current is ~1 ms, and the decay time constant is 10 ms (Banks et al. 1998; Pearce 1993; Traub et al. 1999). In simulations where the effects of synaptic time constants are assessed, the scaling factor ϕ_{syn} is varied, without changing the steady-state mean synaptic currents.

The network connectivity is all-to-all, the summated synaptic current is normalized by the number N of presynaptic cells. Typical network simulations used $N = 400$, except for Fig. 4*C* where $N = 4{,}000$. Numerical simulations were carried out using a fourth-order Runge-Kutta algorithm.

Population activity and coherence index

The network activity is measured by the instantaneous firing rate $R(t)$ as follows. The time is divided into small bins ($\Delta t = 2$ ms). Then

$$R(t) = \frac{\text{total number of spikes in } (t, t + \Delta t)}{N\Delta t}$$

Its mean and variance, averaged over a long time T, are given by

$$\mu_R = \lim_{T\to\infty} \frac{1}{T}\int_0^T R(t)dt; \quad \sigma_R^2 = \lim_{T\to\infty} \frac{1}{T}\int_0^T (R(t) - \mu_R)^2 dt$$

A "coherence index" is defined as the ratio between the SD and the mean of $R(t)$, σ_R/μ_R. For example, in an asynchronous state, $R(t)$ would be constant in time and equal to the firing rate of each individual cell. In that case the coherence index is zero. A coherent network oscillation would be reflected by a rhythmic time course of $R(t)$, and a large coherence index value.

The population rhythmic frequency is determined by the power spectrum of $R(t)$.

RESULTS

Intrinsic membrane oscillations in the model of septal GABAergic neurons

Our model of septal GABAergic neurons reproduces the characteristic electrophysiological profile of noncholinergic (putative GABAergic) cells in BF (Alonso et al. 1996) and MS (Serafin et al. 1996). It displays a temporal pattern of intrinsic rhythmic discharge characterized by recurrent "clusters" of spikes interspersed with subthreshold membrane potential oscillations. The frequencies for both subthreshold oscillations and intra-cluster firing are similar (~40 Hz), and spike clusters repeat rhythmically at ~5 Hz. A simulation example is compared with an intracellular trace in Fig. 1*B*, showing the agreement between the model and a biological neuron.

In Fig. 2*A*, the membrane potential is initially hyperpolarized at -80 mV. On application of a depolarizing current pulse, a long delay with superimposed subthreshold oscillations precedes spiking (see Fig. 1*A* for data). Such a depolarizing delay cannot be elicited if the current pulse is applied from a membrane potential positive to -60 mV, in agreement with the experimental observation (Alonso et al. 1996). The ramp occurs because at -80 mV, the voltage-gated I_{KS} is de-inactivated. In response to current pulse, I_{KS} inactivates slowly (slow decay of the inactivation variable q in Fig. 2*A*), and the cell starts to fire action potentials only when I_{KS} is sufficiently inactivated.

The subthreshold membrane rhythmic fluctuations (near -55 mV) are generated by the interplay between two counteracting currents: the modest window current of the I_{Na} in the subthreshold voltage range (Fig. 2*C*), which provides a fast positive feedback to the membrane potential, and the somewhat slower low-threshold outward I_{KS}. Thus the oscillation is dependent on I_{Na} and sensitive to TTX (Serafin et al. 1996). The oscillation frequency (40–60 Hz) is controlled by the *activation* time constant of I_{KS} as well as the passive mem-

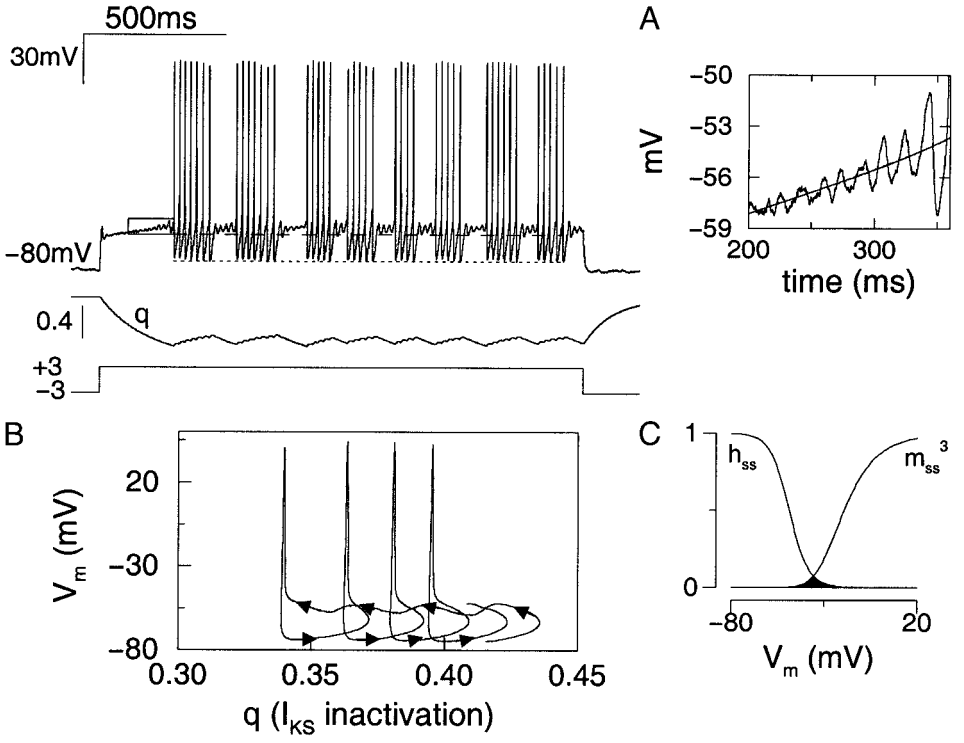

FIG. 2. Characteristic behavior of a septal GABAergic model neuron. *A*: when depolarized from −80 mV, the cell displays a long delay to spike firing (compare with data in Fig. 1*A*), when the I_{KS} inactivates (q slowly decays). After the delay, the slow inactivation process of the I_{KS} induces rhythmic switching between clusters of spikes with deepened afterhyperpolarizations and subthreshold oscillations riding on a depolarizing ramp. *Inset*: enlarged ramp period. Noise amplifies subthreshold oscillations (monotonic curve corresponds to the case without noise). *B*: the membrane potential is plotted against the inactivation variable q of the I_{KS}, showing that q increases during a cluster of spikes, and decreases during a subthreshold episode. *C*: the steady-state curves for the activation and inactivation of the I_{Na}, showing a small window current.

brane time constant. The membrane oscillations are amplified by the presence of noise (Fig. 2*A*, *inset*). Following the depolarizing ramp, the neuron fires a cluster of spikes when I_{KS} de-inactivates and accumulates (Fig. 2*A*, *bottom*), therefore spike afterhyperpolarization gradually becomes larger, eventually preventing the cell from further emitting action potentials. During the following episode of subthreshold oscillations, on the other hand, the I_{KS} gradually inactivates and decreases (Fig. 2*A*, *bottom*), resulting in a progressive depolarization that leads to the spike threshold and the next cluster event. The dynamical interplay between membrane potential and the I_{KS} is also visualized in Fig. 2*B*, where V is plotted against the I_{KS} inactivation variable q: q increases (arrows to the right) during a cluster of spikes, whereas q decreases (arrows to the left) during subthreshold oscillations.

When constant depolarizing current is applied to the model, subthreshold oscillations occur always together with spiking (Fig. 3*A*). With increasing amplitude of injected current, the number of spikes per cluster increases, and spike firing becomes dominant over subthreshold oscillatory episodes. The frequencies of the subthreshold oscillation and intra-cluster firing are plotted as function of the injected current intensity in Fig. 3*B* (*left*). They remain comparable over the current intensity range, and are within the gamma frequency range (40–60 Hz). The frequency of rhythmic cluster repetition is ~2 Hz for small current intensity, and plateaus at ~5 Hz for larger current intensities (Fig. 3*B*, *right*). All these results are similar to the experimentally observed behaviors of the basal forebrain and medial septal putative GABAergic neurons (Alonso et al. 1996; Serafin et al. 1996). Therefore the model reproduces the salient electrophysiological properties of these cells.

The preferred frequency (5 Hz) for the rhythmic recurrence of spike clusters is determined by the kinetics of the I_{KS} inactivation. To further illustrate this point, the scaling constant τ_{q0} of the I_{KS} inactivation time is systematically varied. With larger τ_{q0} values, the I_{KS} inactivation is slower, and the frequency of rhythmic cluster repetition decreases. For τ_{q0} ranging from 50 to 200 ms (with fixed injected current intensity), the inter-cluster rhythmic frequency varies from 10 to 2.5 Hz (Fig. 3*C*), in the θ (4–10 Hz) frequency range. Therefore the oscillation frequency is a smooth and graded function of the I_{KS} inactivation time constant. We emphasize that this inactivation time constant was not chosen by an "ad hoc" parameter tuning but was based on the experimental measurements of a slowly inactivating K^+ current in cortical (Spain et al. 1991) and thalamic (Huguenard and Prince 1991; McCormick 1991) neurons. Our model predicts that a similar ionic current is present in the septal GABAergic cells and plays an important role in their intrinsic oscillations. Furthermore, in a network, the precise oscillation frequency is not uniquely determined by the properties of single pacemaker neurons but depends also on the synaptic interactions (see following text).

Network of septal GABAergic neurons

We next simulated an interconnected network of such inhibitory model neurons to explore whether lateral collaterals of MS GABAergic cells could lead to population synchronization. In simulations, septal GABAergic cells are activated by injected currents, which mimic excitatory drive by cholinergic neurons in the MS. The intensity of injected current varies from cell to cell according to a Gaussian distribution, with a mean and a SD. As a result of heterogeneity, when uncoupled, neurons display different firing rates (ranging 10–30 Hz). We found that θ oscillations could not be synchronized by mutually inhibitory synaptic interactions mediated by $GABA_A$ receptors (Fig. 4*A*). However, the faster γ-frequency oscillations are coherent in the network, as clearly seen in the rastergram as

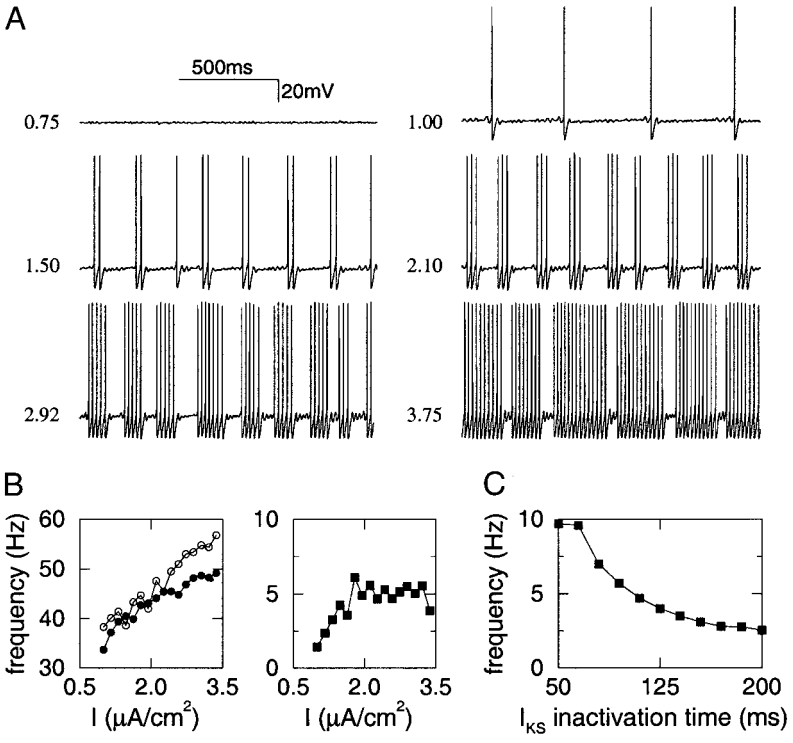

FIG. 3. Temporally nested γ and θ neuronal oscillations. *A*: with increased injected current *I*, subthreshold oscillations occur only as the neuron reaches the firing threshold. The number of spikes per cluster increases with *I*. *B*: the frequencies for subthreshold oscillations (○) and intra-cluster spike firing (●) change in parallel with *I*, ranging from 30 to 60 Hz (*left*); whereas the inter-cluster frequency is ~5 Hz for most of the *I* range (*right*). *C*: with fixed $I = 2.92\ \mu A/cm^2$, the inter-cluster rhythmic frequency is an decreasing function of the scaling factor τ_{q0} of the I_{KS} inactivation time constant, ranging from 10 to 2.5 Hz. (*B* and *C* were calculated in the absence of noise.)

well as by the population activity plot (Fig. 4*A*, *bottom*). We tested different values of the synaptic conductance ($g_{syn} = 0.5-3\ mS/cm^2$) and did not observe network synchronization at theta frequency even with strong synaptic coupling (data not shown).

These observations are consistent with the previous theoretical finding that synaptic inhibition is generally capable of synchronizing oscillatory GABAergic neurons, provided that the synaptic time constant is sufficiently long relative to the oscillation period (Wang and Buzsáki 1996; Wang and Rinzel 1992; Whittington et al. 1995). For $GABA_A$ receptor channels, the decay time constant is ~10 ms (Pearce 1993), suitably long compared with the period of the γ rhythm (≃25 ms) but too short for the θ rhythm (period ≃ 100 ms). We also tested whether slower synapses, such as those mediated by slow $GABA_A$ receptors ($\tau_{syn} \sim 50$ ms) (Banks et al. 1998; Pearce 1993) or by $GABA_B$ receptors ($\tau_{syn} \sim 200$ ms) (Otis et al. 1993), could synchronize the network. Surprisingly, with fixed coupling strength (synaptic conductance), a slower τ_{syn} does not lead to a population synchronization (Fig. 4*B*). On the contrary, the network coherence decreases dramatically with increased τ_{syn} (Fig. 4*C*). Therefore theta rhythm is still not synchronized.

Network of septally projecting GABAergic neurons in hippocampus

It thus appears that even though cluster firing neurons display pacemaker properties, they cannot be synchronized by recurrent synaptic inhibitory connections. We then investigated whether synchronization could be realized with the addition of a second class of GABAergic neurons. Our approach was motivated by experimental evidence that the MS and hippocampus are reciprocally connected in an inhibitory loop. However, in principle our two-population model could be interpreted differently (see DISCUSSION).

The hippocampus-projecting septal GABAergic cells receive feedback projections from a subclass of (calbindin immunoreactive, horizontal O/A) GABAergic cells (Alonso and Köhler 1982; Tóth et al. 1993). We built a model of septally projecting hippocampal GABAergic neurons based on the physiological properties of horizontal O/A cells (Ali and Thomson 1998; Lacaille and Willaims 1990). Endowed with a hyperpolarization-activated cation current I_h (Maccaferri and McBain 1996), the model horizontal O/A interneuron exhibits a depolarizing sag during a hyperpolarizing current pulse, and a suprathreshold postinhibitory rebound triggering a spike at the end of the pulse; whereas on depolarization, the neuron model shows spike-frequency adaptation [Fig. 5*A* compared with Fig. 2*B* in Ali and Thomson (1998)]. We then simulated a population of coupled horizontal O/A interneurons. When they are driven to fire in the θ-frequency range (at 9 Hz), the network cannot be synchronized by inhibitory synaptic interactions mediated by $GABA_A$ receptors. Instead neuronal firings are essentially asynchronous (Fig. 5*B*, rastergram), and the population activity is flat in time (Fig. 5*B*, *bottom*). Slower τ_{syn} fails to produce network synchrony at theta frequency (Fig. 5*C*).

We emphasize that horizontal O/A cells do not have a preferred oscillation frequency unlike septal GABAergic cells. Their firing frequency is a monotonic and essentially linear function of the input current (from 0 to >100 Hz). Furthermore when they are driven to fire at higher rates, in the gamma (~40 Hz) frequency range, the network remains asynchronous (data not shown). This asynchronous behavior at 40 Hz is opposite to that of septal GABAergic neurons (Fig. 4*A*). It is also in contrast to previous studies of networks of fast spiking GABAergic model neurons (Brunel 2000; Brunel and Hakim

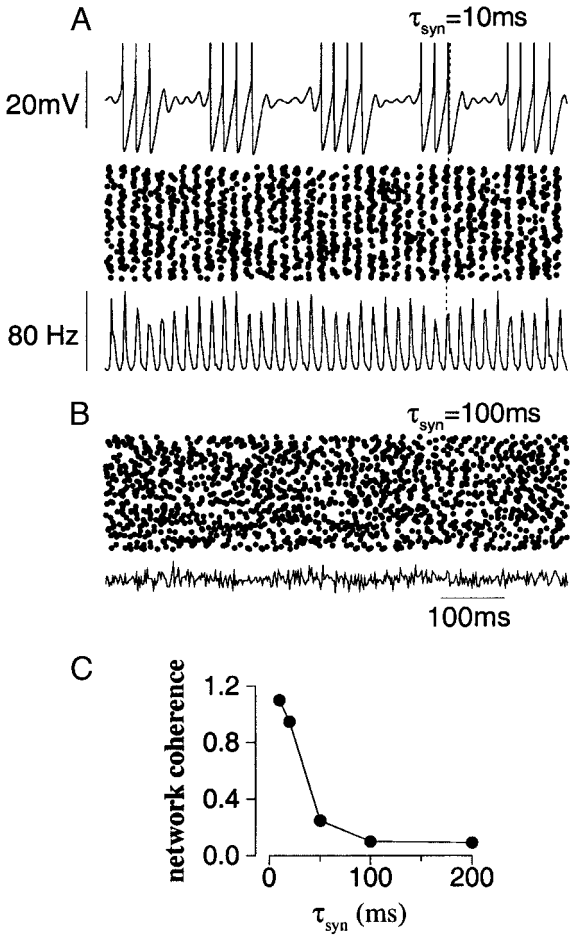

FIG. 4. A network of coupled septal GABAergic model neurons. *A*: input drive varies from cell to cell, according to a Gaussian distribution (mean = 2.5, SD = 0.25 μA/cm^2), so that (when decoupled) individual neurons fire at different rates (10–30 Hz). The fast γ (~40 Hz) oscillations are synchronous among cells, as evidenced by the rastergram (vertical dotted line), and the population activity (*bottom*). However, the slow θ rhythm is not synchronous and invisible in the population activity. (g_{ms-ms} = 0.5 mS/cm^2.) *B*: slower synaptic time constant from 10 to 100 ms leads to desynchronization of the network. *C*: the network coherence decreases dramatically with increasing synaptic time constant.

1999; Chow et al. 1998; Terman et al. 1998; Wang and Buzsáki 1996; White et al. 1998). Note that in the absence of the adaptation currents (I_{Ca} and I_{KCa}) and I_h, the model is identical to Wang and Buzsáki (1996)'s model, which does display synchronous gamma oscillations. Therefore the loss of synchrony at 40 Hz must be due to the inclusion of the additional currents. Crook et al. (1998) have previously shown, in a modeling study, that mutual excitation can synchronize coupled pyramidal neurons with spike-frequency adaptation, whereas the same synaptic interactions lead to desynchronization when the adaptation current is absent. It appears that our model exhibits the flip side of the same phenomenon, in the case of inhibition: synchronization by mutual inhibition is destroyed by spike-frequency adaptation in single neurons.

Reciprocal inhibitory loop between hippocampus and MS

Finally, we simulated a reciprocal circuitry between the medial septal and the hippocampo-septal GABAergic cell populations. The entire network becomes synchronous by the septohippocampal loop (Fig. 6). Interestingly, Both γ oscillations and θ rhythm are synchronous among MS cells, therefore their coherent synaptic output to hippocampus shows the two rhythms interspersed in time (Fig. 6, *bottom*). This is also apparent in the subthreshold membrane oscillations of hippocampal cells, reflecting synchronous rhythmic inhibitory synaptic inputs at γ frequencies (Fig. 6, *top*). Such inter-nested γ and θ rhythms are characteristic of hippocampal activity in vivo during theta episodes (Bragin et al. 1995; Soltész and Deschênes 1993).

In our model, the hippocampal GABAergic cells tend to fire in anti-phase with the MS GABAergic cells (Fig. 6, vertical dotted lines) because the two cell populations are mutually inhibitory and the $GABA_A$ synapses are relatively fast compared with the theta rhythmic period. This is consistent with the reports that hippocampal O/A interneurons tend to fire on the negative phase (Csicsvari et al. 1999), while MS putative GABAergic cells fire mostly on the positive phase (Brazhnik and Fox 1999; Dragoi et al. 1999) of the theta wave recorded in CA1 of the behaving rat.

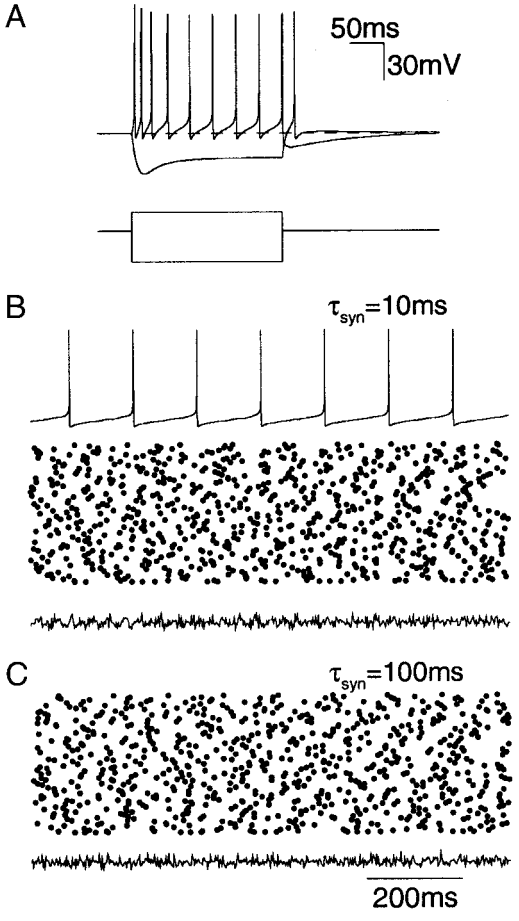

FIG. 5. A network model of septally-projecting, hippocampal horizontal O/A GABAergic neurons. *A*: the single neuron model displays a sag depolarization during a hyperpolarizing current pulse followed by a rebound action potential; and spike-frequency adaptation in response to a depolarizing current pulse. *B*: a population of septally-projecting GABAergic neurons interconnected by $GABA_A$ synapses (τ_{syn} = 10 ms) do not show synchronized oscillation. Neurons fire in an incoherent manner (rastergram), and the population activity is flat in time. *C*: the network is asynchronous even with τ_{syn} = 100 ms. [Input current is distributed according to a Gaussian distribution, mean = 0.5 ± 0.1 (SD) μA/cm^2; $g_{hipp-hipp}$ = 2 mS/cm^2.]

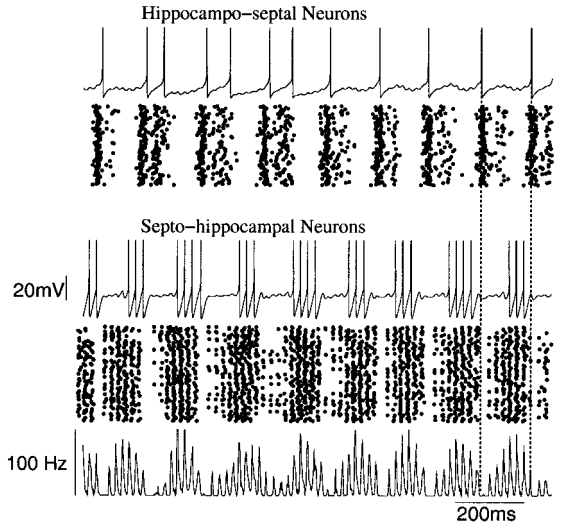

FIG. 6. Coherent θ rhythm in a reciprocal septo-hippocampal loop between medial septal GABAergic cells and hippocampo-septal GABAergic cells. Both fast γ oscillations and slow θ rhythmicity are synchronous (rastergram, population firing rate). The septal and hippocampal GABAergic cell populations fire approximately out-of-phase with each other, consistent with the in vivo data from the awake rat. For better showing the subthreshold membrane potential, the spikes are truncated at −10 mV. (Current drive to septal neurons has a mean = 2.5 ± 0.25; current drive to hippocampal cells has a mean = 1.0 ± 0.2. $g_{ms-hipp} = 2$, $g_{ms-ms} = 0.5$, $g_{hipp-ms} = 1$ mS/cm^2.)

The rhythmic frequency is determined by both the intrinsic oscillation frequency of the septal pacemaker neurons, and synaptic interactions. In the simulation of Fig. 6, both reciprocal connections between the two cell populations and intra-septal connections are present. When the intra-septal inhibition is blocked, the rhythm is slower, 4.2 Hz compared with 6.3 Hz in control (Fig. 7, *A* and *B*). Conversely, an increase in the intra-septal inhibitory conductance leads to a faster network oscillation, up to 9 Hz (Fig. 7*C*). Mutual inhibition between MS cells increases the rhythmic frequency, presumably because it reduces the firing rates of MS cells, so that hippocampal GABAergic cells are inhibited for a shorter period of time per cycle, and the rhythm is accelerated. On the other hand, an increase in the cross-population inhibition in either direction leads to a longer hyperpolarization phase and a slightly decreased rhythmic frequency (Fig. 7, *D–F*).

Again, in our model the hippocampo-septal neurons are not endowed with pacemaker properties and do not have preferred firing frequencies. They can fire one, two, or more spikes per theta cycle in simulations, depending on their excitatory drive. In the hippocampus, the excitatory drive to these cells depends on cholinergic inputs from the septum and recurrent excitation from pyramidal neurons (Blasco-Ibánẽz and Freund 1995). In the model, we varied the mean μ_I and SD σ_I of the Gaussian distribution for the external drive to these cells, whereas the ratio σ_I/μ_I was preserved. Interestingly, with very different firing rates of the hippocampo-septal neurons (6–21 Hz in Fig. 8, *A–D*), the population theta frequency is changed only modestly (Fig. 8*E*) because the theta frequency is largely determined by the pacemaker neurons in the MS. The theta rhythm remains synchronized robustly across the septohippocampal loop.

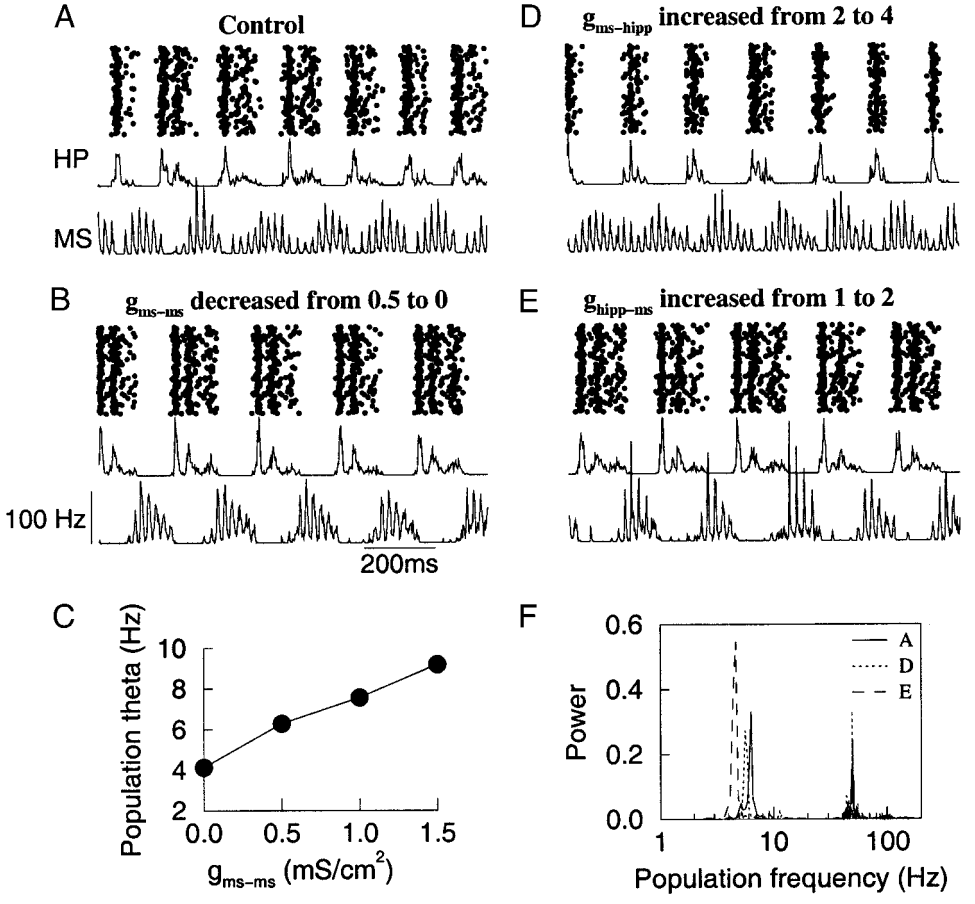

FIG. 7. Dependence of the network theta rhythm on synaptic conductances. *A–D*: rasters from hippocampal neurons (but not from septal cells) and the 2 population firing rates. *A*: control (same as in Fig. 6) with synaptic conductances: $g_{ms-ms} = 0.5$, $g_{ms-hipp} = 2$, $g_{hipp-ms} = 1$ mS/cm^2. *B*: when the intra-septal inhibition is blocked, the theta oscillation is slower. *C*: theta oscillation frequency increases with g_{ms-ms}. *D* and *E*: when the cross-population inhibition is increased in either direction, compared with control, the theta oscillation frequency is decreased slightly compared with control. This is also shown by the power spectrum of the population firing rate (*F*). See text for further discussion.

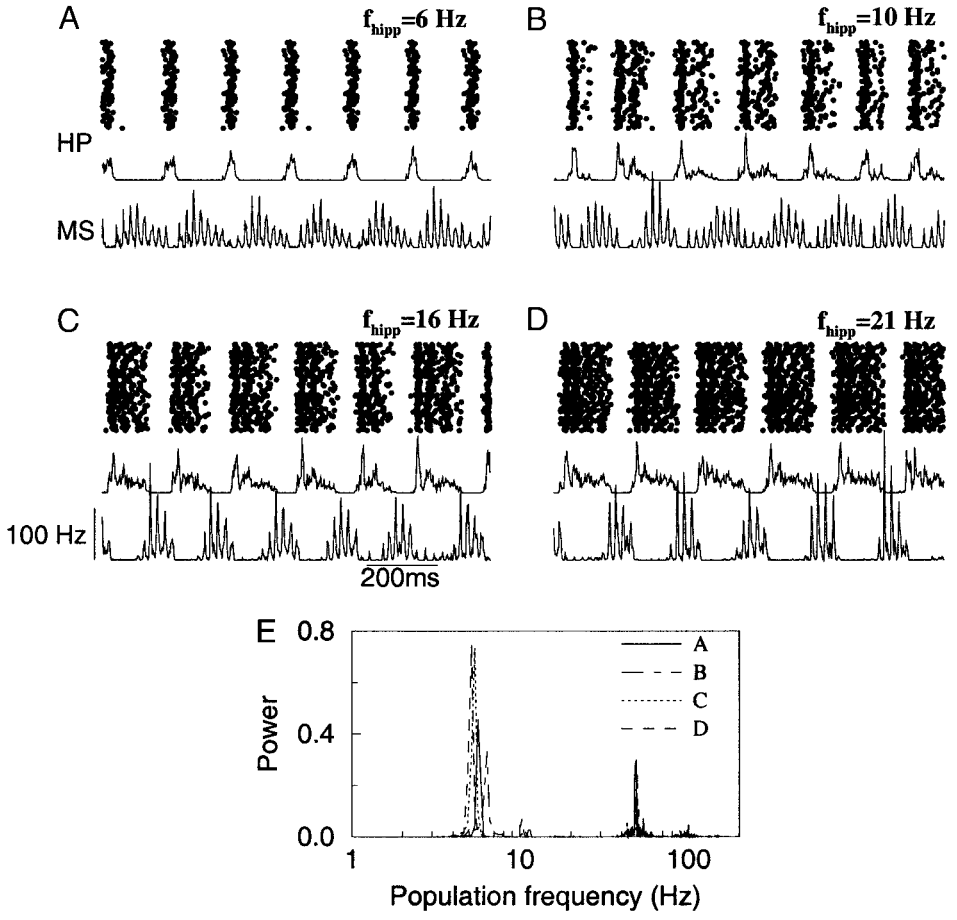

FIG. 8. Hippocampo-septal cells can fire at different frequencies. Same as Fig. 6, with the exception that the mean (μ_I) and SD (σ_I) of the Gaussian distribution for the external drive to hippocampal cells are varied; while σ_I/μ_I is preserved. *A*: $\mu_I = 0.5$, $\sigma_I = 0.1$; *B*: $\mu_I = 1.0$, $\sigma_I = 0.2$; *C*: $\mu_I = 1.5$, $\sigma_I = 0.3$; *D*: $\mu_I = 2.0$, $\sigma_I = 0.4$. The average firing rate of hippocampal cells varies from 6 to 21 Hz. However, the network oscillation frequency (*E*), which is controlled by the medial septal pacemaker cells, is only slightly affected, and the population synchrony remains robust.

DISCUSSION

In this study, we have used a computational approach to test the hypothesis that a population of medial septal GABAergic neurons plays a pacemaker role for the theta rhythmicity in the limbic system. The main findings are twofold. First, the single-cell model reproduces the salient physiological observations from putative septal GABAergic cells in the slices. It gives rise to the prediction that the pacemaker properties observed in those cells depend critically on a low-threshold slowly inactivating potassium current. Second, in network simulations, we found that the synchronization of theta oscillations in these cells can be realized in a hippocampo-septal inhibitory loop. In this scenario, two important in vivo observations from the awake animal can be accounted for: the temporally nested theta and gamma synchronized network oscillations and the anti-phase relationship of the spike firing times between putative septal GABAergic cells and septally projecting hippocampal interneurons.

Ionic basis of intrinsic membrane oscillations in septal GABAergic cells

Our model of MS GABAergic cells is based on recent physiological data of Alonso et al. (1996) and Serafin et al. (1996). According to the model, the temporally nested γ- and θ-frequency membrane oscillations are generated by the interplay between a sodium current and a low-threshold slowly inactivating potassium current. Qualitatively similar cluster firing has been previously studied in neural models and analyzed mathematically (Destexhe et al. 1993; Rinzel 1987; Rinzel and Ermentrout 1998; Wang 1993; Wang and Rinzel 1995). This type of subthreshold membrane oscillations seems to be quite common: they have also been observed in stellate cells in layer II-III of entorhinal cortex (Alonso and Klink 1996; Alonso and Llinás 1989), neocortical neurons (Gutfreund et al. 1995), mitral cells in olfactory bulb (Desmaisons et al. 1999), trigeminal mesencephalic neurons (Pedroarena et al. 1999; Wu et al. 2001), and magnocellular neurons of the hypothalamic supraoptic nucleus (Boehmer et al. 2000). In all these cases, intrinsic membrane oscillations depend on a sodium current and are abolished by TTX but not by Ca^{2+} channel blockers. On the other hand, in most cases the specific outward currents of critical importance to oscillations remain unidentified. In neocortical cells (3–15 Hz) (Gutfreund et al. 1995) and hypothalamic magnocellular neurons (10–70 Hz) (Boehmer et al. 2000), subthreshold oscillations are abolished by TEA, suggesting a critical role of voltage-gated K^+ currents in the rhythmogenesis. For entorhinal cortex layer II stellate cells, subthreshold oscillations are slow (a few hertz). Evidence suggests that a hyperpolarization-activated cation current I_h rather than a K^+ current plays a major role (Dickson et al. 2000). An I_h mechanism, however, would be too slow to generate subthreshold oscillations in the gamma ($\sim$40 Hz) frequency range, as observed in MS putative GABAergic cells. Moreover, the typical ramp response when depolarized from

hyperpolarization (Fig. 1*A*) strongly suggests the presence of a prominent slowly inactivating K^+ current in those cells.

To test this hypothesis, a minimal model was simulated that contains only one more ion current (the I_{KS}) in addition to the Hodgkin-Huxley-type fast currents for action potential generation. We found that the model reproduces the characteristic features of the γ- and θ-frequency intrinsic membrane oscillations and cluster firing as observed in MS putative GABAergic cells. Note that these neurons are likely endowed with other types of ion channels not included in the present model, which may lead to differences in quantitative details between the model and real cells. Nevertheless, the minimal model approach allowed us to demonstrate a special role played by a low-threshold K^+ current that inactivates with a time constant of 50–200 ms. Among a wide diversity of voltage-gated K^+ currents (Coetzee et al. 1999), such slowly inactivating K^+ currents have been observed in neocortical (Spain et al. 1991), thalamic (Huguenard and Prince 1991; McCormick 1991), and other neuron types. Experimental tests of the I_{KS} hypothesis, by identifying and characterizing such a K^+ current in septal GABAergic neurons, would help to elucidate the cellular basis of these membrane oscillations and their neuromodulation.

Network of pacemaker cells coupled by mutually inhibitory synapses

We simulated a network of coupled GABAergic pacemaker neurons, which were assumed to correspond to the hippocampus-projecting and parvalbumin-containing cells (Freund 1989). We found that $GABA_A$ receptor-mediated synaptic inhibition could only synchronize the network in the γ-frequency range but not for the θ rhythmicity. This agrees with other studies showing that the fast $GABA_A$ inhibition is particularly suited for synchronization of γ oscillations (Chow et al. 1998; Wang and Buzsáki 1996; White et al. 1998). However, even with slow synapses of a time constant $\leq$200 ms, the MS GABAergic neurons could still not be strongly synchronized. If that is the case, then even if septal GABAergic cells interact with each other via slow $GABA_A$ receptor subtypes (Pearce 1993) or via $GABA_B$ receptors (Margeta-Mitrovic et al. 1999), their theta oscillations would still not be synchronized within the population. This is in contrast to model studies where neuronal oscillation (also at 5–10 Hz) originates from a postinhibitory rebound mechanism. In that case, $GABA_B$ synapses could give rise to zero-phase synchronization among coupled neurons (Wang and Rinzel 1992, 1993). Several factors need to be further analyzed to account for this difference. In particular, whether mutual inhibition can synchronize a GABAergic neural network likely depends on the intrinsic properties of single neurons. Indeed, the addition of a slow potassium current to model neurons can completely alter a network's synchronization properties given the same synaptic mechanism (Crook et al. 1998). It would be of interest to investigate this issue in more detail in the case of septal GABAergic neurons and to determine how the synchronization properties depend on the presence of the I_{KS}. Furthermore it is conceivable that in some parameter regimes either fast or slow synapses could lead to network synchronization, which is nevertheless not robust in the presence of network heterogeneity (our simulated network has a significant heterogeneity, the firing rates of uncoupled neurons range from 10 to 30 Hz).

Can the MS alone generate coherent theta rhythm?

At present, there is no convincing experimental evidence that an isolated MS is capable of producing coherent theta oscillations. It is an open question as to what extent the observed synchronization among MS cells (Branzhnik and Fox 1999; Gogolák et al. 1968) depends on the hippocampo-septal feedback projections. This question deserves to be revisited experimentally. During lesion of the fimbria-fornix pathway, network synchrony within MS could be assessed by either cross-correlation analysis of neural pairs or local field measurements. One could also investigate whether an isolated MS network in in vitro slices is capable of producing synchronous oscillations at theta frequency.

In the absence of adequate evidence, one can only speculate on candidate synchronization mechanisms that would depend on additional neural populations in the MS. One possibility involves other subclasses of GABAergic cells in MS that contain calbindin or calretinin (Kiss et al. 1997). Heterogenous populations of noncholinergic (putative GABAergic cells) are also consistent with data from slice physiology (Griffith 1988; Markram and Segal 1990; Morris et al. 1999) and recordings from behaving animals (Dragoi et al. 1999; Gaztelu and Bũno 1982; King et al. 1998). It is unknown whether these distinct GABAergic cell populations are interconnected and whether their interactions give rise to network synchronization. Indeed, our results from two-population simulations could have an entirely different interpretation: the second population of GABAergic neurons could be intrinsic to the MS rather than the septally projecting cells in the hippocampus. In this scenario, synchronization would be realized within the MS, through synaptic interactions between two or more subclasses of GABAergic cells.

Moreover, interactions between the GABAergic cells and cholinergic cells also remain to be elucidated. There is no doubt that cholinergic excitation provides an important drive to GABAergic cells. However, muscarinic receptor-mediated cholinergic transmission would seem to be too slow for temporal synchronization at theta frequency. Therefore in order for the cholinergic synapses to be important to theta synchronization, it must be at least partly mediated by fast nicotinic receptors. Physiological evidence for postsynaptic nicotinic receptors in GABAergic cells within the MS is lacking. For this reason, we have chosen not to investigate this scenario in the present model study. Instead, cholinergic neurons in MS were not explicitly included; their action was mimicked by tonic excitatory drives to simulated GABAergic cells. It remains to be seen, by future experimental and theoretical studies, whether a synaptic circuitry that embraces both GABAergic and cholinergic cell populations could lead to synchronicity in the MS.

Synchronization by septohippocampal reciprocal loop

Motivated by the anatomically well-established reciprocal connections between the MS and the hippocampus, we considered the possibility that network synchronization relies on this inhibitory synaptic loop. In our model, an isolated network of (septally projecting) GABAergic O/A cells cannot be synchronized by fast synaptic inhibition at gamma frequency, in contrast to previous model studies (Chow et al. 1998; Wang

and Buzsáki 1996; White et al. 1998; Whittington et al. 1995). Nor can the network be synchronized at theta frequency by slow synaptic inhibition, in contrast to the recent model proposed by White et al. (2000). The asynchronous behavior of this inhibitory network is, again, likely due to the spike-frequency adaptation property of single O/A cells (Crook et al. 1998) and the effects of network heterogeneity.

When the two populations of GABAergic cells are connected together through a reciprocal loop, however, the entire network can easily be synchronized. The synchronization at theta frequency is robust in the presence of heterogeneities. We expect that the synchronization will remain robust even in the case of sparse connectivity (another form of heterogeneity), instead of all-to-all connectivity, as long as the number of synapses per cell is larger than a critical value (Golomb and Hansel 2000; Wang and Buzsáki 1996).

In our model, the two GABAergic cell populations fire out of phase during a theta cycle as expected for two reciprocally inhibitory neural populations coupled by fast synapses (Marder and Calabrese 1996; Wang and Rinzel 1992). This is consistent with the recording data from the awake rat (Brazhnik and Fox 1999; Dragoi et al. 1999); it is also in consonance with the idea that GABAergic septohippocampal projection suppresses spike discharges in hippocampal interneurons, thereby disinhibiting pyramidal cells (Freund and Antal 1988; Tóth et al. 1997). Intuitively, an out-of-phase oscillation occurs as follows. Septal pacemaker cells fire repetitive clusters of spikes. A cluster terminates as a result of the I_{KS} increase ("neuronal fatigue"), so that the hippocampal neurons are "released" from septal inhibition and fire. The I_h in these cells may also contribute to the "rebound" response. Afterward, septal cells slowly recover from hyperpolarization while I_{KS} inactivates and eventually "escape" from decaying inhibition mediated by the hippocampo-septal cells. And the cycle starts over again. A detailed mathematical analysis of the synchronization mechanisms in the two population loop is outside the scope of this paper and will be reported elsewhere.

Recently White et al. (2000) presented a new model of synchronous oscillations generated intrinsically in the hippocampus. Their model also includes two interconnected populations of GABAergic neurons; but neither of the two displays pacemaker properties. Both populations are tonically firing cells; they differ in the kinetic properties of their inhibitory postsynaptic currents ($GABA_{A,\,fast}$ with $\tau = 9$ ms, and $GABA_{A,\,slow}$ with $\tau = 50$ ms, respectively). The model displays both theta and gamma oscillations. However, the theta rhythm produced by the slow subtype of $GABA_A$ synapses (Banks et al. 1998; Pearce 1993) is rather fragile and is easily destroyed by a small amount of network heterogeneity. In the latter case, the $GABA_{A,\,slow}$ mechanism can greatly amplify a periodic input at theta frequency, presumably from the MS, even though the oscillatory signal is weak and phase-dispersed. Therefore the MS is still required as a pacemaker for the hippocampal theta. Other theoretical work has also explored the role of resonance in hippocampal theta, which is driven by a periodic septal input (Borisyuk and Hoppensteadt 1999; Orban et al. 2001).

The present study addressed the question of how the putative septal pacemaker neurons are synchronized in the first place. The hypothesized synchronizing role of septohippocampal loop can be tested experimentally. First, further work is needed to compare the model with data concerning the relative theta phases of firing times between hippocampal cells and septo-hippocampal GABAergic neurons. Second, our result raises a critical question of whether an isolated MS is capable of generating coherent theta oscillations by itself. This question could be studied in vivo by measuring the synchronization properties of septal pacemaker neurons when the hippocampal theta is abolished by fimbria-fornix lesion; and it could also conceivably be investigated in slice preparations. Third, the possible role of the hippocampo-septal feedback projections in theta rhythm synchronization may be tested by selectively disabling this particular pathway.

Finally, it should be noted that the septohippocampal loop is not the only possible substrate for such a "half-center oscillator" mechanism. As mentioned earlier, another possibility involves two different subclasses of GABAergic cells inside the MS. Moreover, two-way connections also exist between the MS and the entorhinal cortex, but it is unknown whether this pathway also encompasses a reciprocal inhibitory loop. Answers to this question would be especially interesting in light of the fact that entorhinal afferents are believed to play the most important role in the current generation of extracellular field theta in the hippocampus and that entorhinal lesions render the remaining hippocampal theta oscillation atropine-sensitive (Buzsáki 2001; Buzsáki et al. 1983).

I am grateful to A. Alonso for stimulating and fruitful discussions on his data and on modeling of septal single neurons. I also thank T. Freund, G. Buzsáki, and C. McBain for helpful discussions.

This work was supported by the National Institute of Mental Health, the Alfred P. Sloan Foundation, and the W. M. Keck Foundation.

REFERENCES

ALI AB AND THOMSON AM. Facilitating pyramid to horizontal oriens-alveus interneurone inputs: dual intracellular recordings in ss of rat hippocampus. *J Physiol (Lond)* 507: 185–199, 1998.

ALONSO A, KHATEB A, FORT P, JONES BE, AND MÜHLETHALER M. Differential oscillatory properties of cholinergic and non-cholinergic nucleus basalis neurons in guinea pig brain slice. *Eur J Neurosci* 8: 169–182, 1996.

ALONSO A AND KLINK R. Differential electroresponsiveness of stellate and pyramidal-like cells of medial entorhinal cortex layer II. *J Neurophysiol* 70: 128–143, 1993.

ALONSO A AND KÖHLER C. Evidence for separate projections of hippocampal pyramidal and non-pyramidal neurons to different parts of the septum in the rat brain. *Neurosci Lett* 31: 209–214, 1982.

ALONSO A AND LLINÁS RR. Subthreshold Na^+-dependent theta-like rhythmicity in stellar cells of entorhinal cortex layer II. *Nature* 342: 175–177, 1989.

ANDERSEN P, BLAND HB, MYHRER T, AND SCHWARTZKROIN PA. Septo-hippocampal pathway necessary for dentate theta production. *Brain Res* 165: 13–22, 1979.

APARTIS E, POINDESSOUS-JAZAT FR, LAMOUR YA, AND BASSANT MH. Loss of rhythmically bursting neurons in rat medial septum following selective lesion of septohippocampal cholinergic system. *J Neurophysiol* 79: 1633–1642, 1998.

BANKS MI, LI T-B, AND PEARCE RA. The synaptic basis of GABAA, slow. *J Neurosci* 18: 1305–1317, 1998.

BLAND BH. The physiology and pharmacology of hippocampal formation theta rhythms. *Prog Neurobiol* 26: 1–54, 1986.

BLASCO-IBÁÑEZ JM AND FREUND TF. Synaptic input of horizontal interneurons in stratum oriens of the hippocampal CA1 subfield: structural basis of feed-back activation. *Eur J Neurosci* 7: 2170–2180, 1995.

BOEHMER G, GREFFRATH W, MARTIN E, AND HERMANN S. Subthreshold oscillation of the membrane potential in magnocellular neurones of the rat supraoptic nucleus. *J Physiol (Lond)* 526: 115–128, 2000.

BORISYUK R AND HOPPENSTEADT F. Oscillatory models of the hippocampus: a study of spatio-temporal patterns of neural activity. *Biol Cybern* 81: 359–371, 1999.

BRAGIN A, JANDÓ G, NÁDASDY Z, HETKE J, WISE K, AND BUZSÁKI G. Gamma (40–100 Hz) oscillation in the hippocampus of the behaving rat. *J Neurosci* 15: 47–60, 1995.

BRAZHNIK ES AND FOX SE. Action potentials and relations to the theta rhythm of medial septal neurons in vivo. *Exp Brain Res* 127: 244–258, 1999.

BRASHEAR HR, ZABORSZKY L, AND HEIMER L. Distribution of GABAergic and cholinergic neurons in the rat diagonal band. *Neuroscience* 17: 439–451, 1986.

BRUNEL N. Dynamics of sparsely connected networks of excitatory and inhibitory spiking neurons. *J Comput Neurosci* 8: 183–208, 2000.

BRUNEL N AND HAKIM V. Fast global oscillations in networks of integrate-and-fire neurons with low firing rates. *Neural Comput* 11: 1621–1671, 1999.

BUZSÁKI G. A two-stage model of memory trace formation: a role for "noisy" brain states. *Neuroscience* 31: 551–570, 1989.

BUZSÁKI G. Theta oscillations in the hippocampus. *Neuron*. In press.

BUZSÁKI G, LEUNG L, AND VANDERWOLF CH. Cellular bases of hippocampal EEG in the behaving rat. *Brain Res Rev* 6: 139–171, 1983.

CHOW CC, WHITE JA, RITT J, AND KOPELL N. Frequency control in synchronized networks of inhibitory neurons. *J Comput Neurosci* 5: 407–420, 1998.

COBB SR, BUHL EH, HALASY K, PAULSEN O, AND SOMOGYI P. Synchronization of neuronal activity in hippocampus by individual GABAergic interneurons. *Nature* 378: 75–78, 1995.

COETZEE WA, AMARILLO Y, CHIU J, CHOW A, LAU D, MCCORMACK T, MORENO H, NADAL MS, OZAITA A, POUNTNEY D, SAGANICH M, VEGA-SAENZ DE MIERA E, AND RUDY B. Molecular diversity of K^+ channels. *Ann NY Acad Sci* 868: 233–295, 1999.

COLE AE AND NICOLL RA. Characterization of a slow cholinergic post-synaptic potential recorded in vitro from rat hippocampal pyramidal cells. *J Physiol (Lond)* 352: 173–188, 1984.

CROOK SM, ERMENTROUT GB, AND BOWER JM. Spike frequency adaptation affects the synchronization properties of networks of cortical oscillators. *Neural Comput* 10: 837–854, 1998.

CSICSVARI J, HIRASE H, CZURKO A, MAMIYA A, AND BUZSAKI G. Oscillatory coupling of hippocampal pyramidal cells and interneurons in the behaving rat. *J Neurosci* 19: 274–287, 1999.

DESMAISONS D, VINCENT JD, AND LLEDO PM. Control of action potential timing by intrinsic subthreshold oscillations in olfactory bulb output neurons. *J Neurosci* 19: 10727–10737, 1999.

DESTEXHE A, MCCORMICK DA, AND SEJNOWSKI TJ. A model for 8–10 Hz spindling in interconnected thalamic relay and reticular neurons. *Biophys J* 65: 2473–2477, 1993.

DICKSON CT, MAGISTRETTI J, SHALINSKY MH, FRANSEN E, HASSELMO ME, AND ALONSO A. Properties and role of I_h in the pacing of subthreshold oscillations in entorhinal cortex layer II neurons. *J Neurophysiol* 83: 2562–2579, 2000.

DRAGOI G, CARPI D, RECCE M, CSICSVARI J, AND BUZSAKI G. Interactions between hippocampus and medial septum during sharp waves and theta oscillation in the behaving rat. *J Neurosci* 19: 6191–6199, 1999.

FISCHER Y, GÄHWILER BH, AND THOMPSON SM. Activation of intrinsic hippocampal theta oscillations by acetylcholine in rat septo-hippocampal cocultures. *J Physiol (Lond)* 519: 405–413, 1999.

FREUND TF. GABAergic septohippocampal neurons contain parvalbumin. *Brain Res* 478: 375–381, 1989.

FREUND TF AND ANTAL M. GABA-containing neurons in the septum control inhibitory interneurons in the hippocampus. *Nature* 336: 170–173, 1988.

GÄHWILER BH AND BROWN DA. Functional innervation of cultured hippocampal neurones by cholinergic afferents from co-cultured septal explants. *Nature* 313: 577–579, 1985.

GAZTELU JM AND BUNO W JR. Septo-hippocampal relationships during EEG theta rhythm. *Electroencephalogr Clin Neurophysiol* 54: 375–387, 1982.

GOGOLÁK G, STUMPF C, PETSCHE H, AND STERC J. The firing pattern of septal neurons and the form of the hippocampal theta wave. *Brain Res* 7: 201–207, 1968.

GOLOMB D AND HANSEL D. The number of synaptic inputs and the synchrony of large, sparse neuronal networks. *Neural Comput* 12: 1095–1139, 2000.

GREEN JD AND ARDUNI AA. Hippocampal electrical activity in arousal. *J Neurophysiol* 17: 533–557, 1954.

GRIFFITH WH. Membrane properties of cell types within guinea pig basal forebrain nuclei in vitro. *J Neurophysiol* 59: 1590–1612, 1988.

GRITTI I, MAINVILLE L, AND JONES BE. Codistribution of GABA- with acetylcholine-synthesizing neurons in the basal forebrain of the rat. *J Comp Neurol* 329: 438–457, 1993.

GUTFREUND Y, YAROM Y, AND SEGEV I. Subthreshold oscillations and resonant frequency in guinea-pig cortical neurons: physiology and modelling. *J Physiol (Lond)* 483: 621–640, 1995.

HELMCHEN F, IMOTO K, AND SAKMANN B. Ca^{2+} buffering and action potential-evoked Ca^{2+} signaling in dendrites of pyramidal neurons. *Biophys J* 70: 1069–1081, 1996.

HUGUENARD JR AND PRINCE DA. Slow inactivation of a TEA-sensitive K current in acutely isolated rat thalamic relay neurons. *J Neurophysiol* 66: 1316–1328, 1991.

HUERTA PT AND LISMAN JE. Heightened synaptic plasticity of hippocampal CA1 neurons during a cholinergically induced rhythmic state. *Nature* 364: 723–725, 1993.

HUTCHEON B AND YAROM Y. Resonance, oscillation and the intrinsic frequency preferences of neurons. *Trends Neurosci* 23: 216–222, 2000.

KAHANA MJ, SEKULER R, CAPLAN JB, KIRSCHEN M, AND MADSEN JR. Human theta oscillations exhibit task dependence during virtual maze navigation. *Nature* 399: 781–784, 1999.

KING C, RECCE M, AND O'KEEFE J. The rhythmicity of cells of the medial septum/diagonal band of Broca in the awake freely moving rat: relationships with behaviour and hippocampal theta. *Eur J Neurosci* 10: 464–477, 1998.

KISS J, MAGLOCZKY Z, SOMOGYI J, AND FREUND TF. Distribution of calretinin-containing neurons relative to other neurochemically identified cell types in the medial septum of the rat. *Neuroscience* 78: 399–410, 1997.

KRAMIS R, VANDERWOLF CH, AND BLAND BH. Two types of hippocampal rhythmical slow activity in both the rabbit and the rat: relations to behavior and effects of atropine, diethyl ether, urethane, and pentobarbital. *Exp Neurol* 49: 58–85, 1975.

LACAILLE JC AND WILLIAMS S. Membrane properties of interneurons in stratum oriens-alveus of the CA1 region of rat hippocampus in vitro. *Neuroscience* 36: 349–359, 1990.

LEE MG, CHROBAK JJ, SIK A, WILEY RG, AND BUZSÁKI G. Hippocampal theta activity following selective lesion of the septal cholinergic system. *Neuroscience* 62: 1033–1047, 1994.

LLINÁS RR, GRACE AA, AND YAROM Y. *In vitro* neurons in mammalian cortical layer 4 exhibit intrinsic oscillatory activity in the 10- to 50-Hz frequency range. *Proc Natl Acad Sci USA* 88: 897–901, 1991.

MACCAFERRI G AND MCBAIN CJ. The hyperpolarization-activated current (Ih) and its contribution to pacemaker activity in rat CA1 hippocampal stratum oriens-alveus interneurones. *J Physiol (Lond)* 497: 119–130, 1996.

MACVICAR BA AND TSE FWY. Local neuronal circuitry underlying cholinergic rhythmical slow activity in area CA3 of rat hippocampal slices. *J Physiol (Lond)* 417: 197–212, 1989.

MARDER E AND CALABRESE R. Principles of rhythmic motor pattern generation. *Physiol Rev* 76: 687–717, 1996.

MARGETA-MITROVIC M, MITROVIC I, RILEY RC, JAN LY, AND BASBAUM AI. Immunohistochemical localization of GABA(B) receptors in the rat central nervous system. *J Comp Neurol* 405: 299–321, 1999.

MARKRAM H AND SEGAL M. Electrophysiological characteristics of cholinergic and non-cholinergic neurons in the rat medial septum-diagonal band complex. *Brain Res* 513: 171–174, 1990.

MCCORMICK DA. Functional properties of a slowly inactivating potassium current I_{AS} in guinea pig dorsal lateral geniculate relay neurons. *J Neurophysiol* 66: 1176–1189, 1991.

MORRIS NP, HARRIS SJ, AND HENDERSON Z. Parvalbumin-immunoreactive, fast-spiking neurons in the medial septum/diagonal band complex of the rat: intracellular recordings in vitro. *Neuroscience* 92: 589–600, 1999.

O'KEEFE J AND RECCE ML. Phase relationship between hippocampal place units and the EEG theta rhythm. *Hippocampus* 3: 317–330, 1993.

ORBAN G, KISS T, LENGYEL M, AND ERDI P. Hippocampal rhythm generation: gamma-related theta-frequency resonance in CA3 interneurons. *Biol Cybern* 84: 123–132, 2001.

OTIS TS, DE KONINCK Y, AND MODY I. Characterization of synaptically elicited GABAB responses using patch-clamp recordings in rat hippocampal slices. *J Physiol (Lond)* 463: 391–407, 1993.

PEARCE RA. Physiological evidence for two distinct $GABA_A$ responses in rat hippocampus. *Neuron* 10: 189–200, 1993.

PEDROARENA CM, POSE IE, YAMUY J, CHASE MH, AND MORALES FR. Oscillatory membrane potential activity in the soma of a primary afferent neuron. *J Neurophysiol* 82: 1465–1476, 1999.

PETSCHE H, STUMPF C, AND GOGOLAK G. The significance of the rabbit's septum as a relay station between the midbrain and the hippocampus. I. The control of hippocampal arousal activity by the septum cells. *Electroencephalogr Clin Neurophysiol* 19: 25–33, 1962.

PIKE FG, GODDARD RS, SUCKLING JM, GANTER P, KASTHURI N, AND PAULSEN O. Distinct frequency preferences of different types of rat hippocampal neurones in response to oscillatory input currents. *J Physiol (Lond)* 529: 205–213, 2000.

RINZEL J. A formal classification of bursting mechanisms in excitable systems. In: *Proceedings of the International Congress of Mathematicians*, edited by Gleason AM. Providence, RI: American Mathematical Society, 1987, p. 1578–1594.

RINZEL J AND ERMENTROUT GB. Analysis of neural excitability and oscillations. In: *Methods in Neural Modeling*, edited by Koch C and Segev I. Cambridge, MA: MIT Press, 1998, pp. 251–291.

SERAFIN M, WILLIAMS S, KHATEB A, FORT P, AND MÜHLETHALER M. Rhythmic firing of medial septum non-cholinergic neurons. *Neuroscience* 75: 671–675, 1996.

SKAGGS WE, MCNAUGHTON BL, WILSON MA, AND BARNES CA. Theta phase procession in hippocampal neuronal populations and the compression of temporal sequences. *Hippocampus* 6: 149–172, 1996.

SOLTÉSZ I AND DESCHÊNES M. Low- and high-frequency membrane potential oscillations during theta activity in CA1 and CA3 pyramidal neurons of the rat hippocampus under ketamine-xylazine anesthesia. *J Neurophysiol* 70: 97–116, 1993.

SPAIN WJ, SCHWINDT PC, AND CRILL WE. Two transient potassium currents in layer V pyramidal neurones from cat sensorimotor cortex. *J Physiol (Lond)* 434: 591–607, 1991.

STEWART M AND FOX SE. Do septal neurons pace the hippocampal theta rhythm? *Trends Neurosci* 13: 163–168, 1990.

STUMPF C. The fast component in the electrical activity of rabbit's hippocampus. *Electroencephalogr Clin Neurophysiol* 18: 477–486, 1965.

TERMAN D, KOPELL N, AND BOSE A. Dynamics of two mutually coupled slow inhibitory neurons. *Physica D* 117: 241–275, 1998.

TÓTH K, BORTHEGYI Z, AND FREUND TF. Postsynaptic targets of GABAergic hippocampal neurons in the medial septum-diagonal band of Broca complex. *J Neurosci* 13: 3712–3724, 1993.

TÓTH K AND FREUND TF. Calbindin D28k-containing nonpyramidal cells in the rat hippocampus: their immunoreactivity for GABA and projection to the medial septum. *Neuroscience* 49: 793–805, 1992.

TÓTH K, FREUND TF, AND MILES R. Disinhibition of rat hippocampal pyramidal cells by GABAergic afferents from the septum. *J Physiol (Lond)* 500: 463–474, 1997.

TRAUB RD, JEFFERYS JGR, AND WHITTINGTON MA. *Fast Oscillations in Cortical Circuits.* Cambridge, MA: MIT Press, 1999.

TRAUB RD, MILES R, AND BUZSAKI G. Computer simulation of carbachol-driven rhythmic population oscillations in the CA3 region of the in vitro rat hippocampus. *J Physiol (Lond)* 451: 653–672, 1992.

VANDERWOLF CH. Hippocampal electrical activity and voluntary movement in the rat. *Electroencephalogr Clin Neurophysiol* 26: 407–418, 1969.

VINOGRADOVA OS. Expression, control, and probable functional significance of the neuronal theta-rhythm. *Prog Neurobiol* 45: 523–583, 1995.

WANG X-J. Ionic basis for intrinsic 40 Hz neuronal oscillations. *Neuroreport* 5: 221–224, 1993.

WANG X-J. Calcium coding and adaptive temporal computation in cortical pyramidal neurons. *J Neurophysiol* 79: 1549–1566, 1998.

WANG X-J AND BUZSÁKI G. Gamma oscillations by synaptic inhibition in a hippocampal interneuronal network. *J Neurosci* 16: 6402–6413, 1996.

WANG X-J AND RINZEL J. Alternating and synchronous rhythms in reciprocally inhibitory model neurons. *Neural Computat* 4: 84–97, 1992.

WANG X-J AND RINZEL J. Spindle rhythmicity in the reticularis thalami nucleus: synchronization among mutually inhibitory neurons. *Neuroscience* 53: 899–904, 1993.

WANG X-J AND RINZEL J. Oscillatory and bursting properties of neurons. In: *The Handbook of Brain Theory and Neural Networks*, edited by Arbib M. Cambridge, MA: MIT Press, 1995, p. 686–691.

WHITE JA, BANKS MI, PEARCE RA, AND KOPELL N. Networks of interneurons with fast and slow γ-aminobutyric acid type A (GABAA) kinetics provide substrate for mixed gamma-theta rhythm. *Proc Natl Acad Sci USA* 97: 8128–8133, 2000.

WHITE JA, CHOW CC, SOTO-TREVINO C, AND KOPELL N. Synchronization and oscillatory dynamics in heterogeneous mutually inhibitory neurons. *J Comput Neurosci* 5: 5–16, 1998.

WHITTINGTON MA, TRAUB RD, AND JEFFREYS JGR. Synchronized oscillations in interneuron networks driven by metabotropic glutamate receptor activation. *Nature* 373: 612–615, 1995.

WILLIAMS JH AND KAUER JA. Properties of carbachol-induced oscillatory activity in rat hippocampus. *J Neurophysiol* 78: 2631–2640, 1997.

WU N, HSIAO C-F, AND CHANDLER SH. Membrane resonance and subthreshold membrane oscillations in mesencephalic V neurons: participants in burst generation. *J Neurosci* 21: 3729–3739, 2001.